Analytical and experimental demonstration of depth of field extension for incoherent imaging system with a standard sinusoidal phase mask

Hui Zhao (赵 惠)* and Yingcai Li (李英才)

Xi'an Institute of Optics and Precision Mechanics, Chinese Academy of Science, Xi'an 710119, China

**Corresponding author: zhaohui@opt.ac.cn*

Received June 24, 2011; accepted September 5, 2011; posted online October 31, 2011

The wavefront coding technique is used to enlarge the depth of field (DOF) of incoherent imaging systems. The key to wavefront coding lies in the design of suitable phase masks. To date, numerous kinds of phase masks are proposed. However, further understanding is needed regarding phase mask with its phase function being in a standard sinusoidal form. Therefore, the characteristics of such a phase mask are studied in this letter. Deriving the defocused optical transfer function (OTF) analytically proves that the standard sinusoidal phase mask is effective in extending the DOF, and actual experiments confirm the numerical results. At the same time, with the Fisher information as a criterion, the standard sinusoidal phase mask shows a higher tolerance to focus errors (especially severe focus errors) than the classical cubic phase mask.

OCIS codes: 110.7348, 110.1758.

doi: 10.3788/COL201210.031101.

Wavefront coding, proposed by Dowski *et al.*[1] in 1995, is a breakthrough in extending the depth of field (DOF) of incoherent imaging systems and the key to wavefront coding lies in the design of phase masks.

The cubic phase mask was first designed in 1995. Since then, numerous phase masks have been studied for wavefront coding system. Such phase masks include the exponential[2], logarithmic[3−5], odd-symmetric quadratic[6], and high-order[7] types. All of these types could be used to extend the DOF. To our knowledge, the sinusoidal phase function described in this letter is not as well understood as the other fundamental functions used to design the required phase masks. In comparison, a function similar to sinusoidal is the cosine, which has received much attention during the past years[8−11].

In our previous research[12], a phase mask with phase function of $ax^4\sin(\omega x)+ay^4\sin(\omega y)$ was designed and named as sinusoidal phase mask. Its performance was compared to three other popular phase masks, and was found capable of enlarging the DOF and ensuring high quality of restored images. However, this sinusoidal phase mask is not in the general form, which can be described by amplitude, angular frequency, and initial phase angle. Thus, the sinusoidal phase mask with phase function defined as $\alpha\sin(\omega x+\theta)+\alpha\sin(\omega y+\theta)$ is investigated in this letter, and renamed as the standard sinusoidal phase mask.

Unlike other phase masks, the phase profile of sinusoidal phase masks has periodicity. If the angular frequency is large enough, the phase function cycle becomes very small and the phase mask becomes similar to a sinusoidal grating. In this case, the phase mask could have spatially dense features and will suffer from chromatic dispersion. Such issue can be avoided by imposing a limit on the angular frequency, to ensure that the phase profile has less than a half cycle within the aperture plane. Hence, the local periodicity will disappear and the chromatic dispersion can be eliminated.

The phase function $[\alpha\sin(\omega x+\theta)+\alpha\sin(\omega y+\theta)]$ of the standard sinusoidal phase mask is clearly separable in two rectangular directions. Therefore, the aperture of the imaging system under discussion is also assumed to be rectangular. Under these circumstances, one dimensional case is enough for the following analysis. With a phase mask added to the aperture plane, the generalized pupil function containing focus errors can be described as

$$P(x)=\frac{1}{\sqrt{2}}\begin{cases}\exp\left\{\mathrm{j}\cdot\left[g(x)+kW_{20}\cdot x^2\right]\right\} & \text{for } |x|\leqslant 1,\\ 0 & \text{otherwise,}\end{cases} \tag{1}$$

where x is the normalized pupil plane coordinate in the horizontal direction and within the range of [–1, 1]; k is the wave number; W_{20} is the defocus aberration constant defined as $W_{20}=[(\pi D^2)/(4\lambda)]\cdot(1/f-1/d_{\mathrm{o}}-1/d_{\mathrm{i}})$[1], where D, f, d_{o}, d_{i}, and λ represent the aperture diameter, focal length, object distance, image distance, and wavelength, respectively; g is the corresponding phase function.

According to the scalar diffraction theory, the defocused OTF can be obtained through autocorrelation of generalized pupil function. This can be written as

$$\begin{aligned}H(u,W_{20})=&\frac{1}{2}\cdot\int_{-(1-|u|/2)}^{1-|u|/2}P(x+u/2)\cdot P^*(x-u/2)\,\mathrm{d}x\\ =&\frac{1}{2}\cdot\int_{-(1-|u|/2)}^{1-|u|/2}\exp\{\mathrm{j}\cdot[2kW_{20}ux\\ &+g(x+u/2)-g(x-u/2)]\}\mathrm{d}x,\end{aligned} \tag{2}$$

where u is the reduced spatial frequency and within the range of [–2, 2].

Replacing g with $\alpha\sin(\omega x+\theta)$, Eq. (2) can be con-

verted to

$$H(u,W_{20}) = \frac{1}{2}\cdot\int_{-(1-|u|/2)}^{1-|u|/2}\exp\{\mathrm{j}\cdot[2kW_{20}ux + 2a\cdot\sin\frac{\omega u}{2}\cdot\cos(\omega x+\theta)]\}\mathrm{d}x. \quad (3)$$

Equation 3 cannot be evaluated by traditional methods. Instead, the method of stationary phase[1,14] should be used. Letting ϕ denote the exponential phase in the integrand of Eq. (2), then Eq. (3) can be approximately evaluated as

$$H(u,W_{20}) = \sqrt{\frac{2\pi}{k\cdot|\phi''(x_\mathrm{s})|}} = \sqrt{\frac{\pi}{\left|a\omega^2\cdot\sin\frac{\omega u}{2}\cdot\sqrt{1-\left(\frac{kuW_{20}}{a\omega\cdot\sin\frac{\omega u}{2}}\right)^2}\right|}} \quad u\neq 0, \quad (4)$$

where ϕ'' is the second-order derivative of ϕ with respect to x. The stationary point x_s is obtained by making the first-order derivative of ϕ with respect to x as zero and should satisfy the condition (A): $\sin(\omega x_\mathrm{s}+\theta) = (kuW_{20})/[a\omega\cdot\sin(\omega u/2)]$.

Equation 4 indicates that the imaging system can be made to be defocus invariant only when the condition (B): $|(kuW_{20})/[a\omega\cdot\sin(\omega u/2)]| << 1$ is satisfied across the operating DOF of the imager. In this case, the OTF will be largely invariant to the defocus aberration constant, thus extending the DOF. However, an underlying constraint exists for the mask parameters α, ω, and θ.

According to the condition (B), the condition (A) can be simplified as following equation and the stationary point x_s can be obtained as

$$\omega x_\mathrm{s}+\theta = 2m\pi + \arcsin\left(\frac{kuW_{20}}{a\omega\cdot\sin\frac{\omega u}{2}}\right) \approx 2m\pi + \frac{kuW_{20}}{a\omega\cdot\sin\frac{\omega u}{2}}, \quad (5)$$

$$x_\mathrm{s} \approx \frac{2m\pi + \frac{kuW_{20}}{a\omega\cdot\sin\frac{\omega u}{2}} - \theta}{\omega}, \quad (6)$$

where m equals 0, ±1, ±2, ±3,$\cdots$.

Using the stationary phase method[14] requires that Eq. (3) is evaluated within the region $x_\mathrm{s}\in[-\varepsilon,\varepsilon]$, where ε is very small. Thus, only one value for x_s is effective in usual cases, and Eq. (6) can be rewritten as

$$x_\mathrm{s} \approx \frac{\frac{kuW_{20}}{a\omega\cdot\sin\frac{\omega u}{2}} - \theta}{\omega}. \quad (7)$$

At the same time, the stationary point should also be within the region of $[-(1-|u|/2),(1-|u|/2)]$. Hence, the relationship between the mask parameters α, ω, and θ can be given as

$$\frac{kuW_{20}}{a\omega\cdot\sin\frac{\omega u}{2}} - \omega\cdot\left(1-\frac{|u|}{2}\right) < \theta < \frac{kuW_{20}}{a\omega\cdot\sin\frac{\omega u}{2}} + \omega\cdot\left(1-\frac{|u|}{2}\right). \quad (8)$$

The analytical derivation clearly indicates that the sinusoidal phase mask can extend the DOF of incoherent imaging systems on the condition that Eq. (8) is satisfied. Optimization should be the first step to assess the sinusoidal phase mask performance. Among all the optimization methods, Fisher imformation based method[2,13] is adopted in this study and simulated annealing is used to obtain the global optimum mask parameters, as given in Table 1. At the same time, Eq. (8) is also incorporated into the optimization procedure as a constraint, which ensures that the optimum mask parameters are consistent with theoretical analysis. Furthermore, as already mentioned, the normalized phase profile within the aperture plane can only have less than half cycle during the optimization of the phase mask to ensure that the phase mask will not suffer from chromatic dispersion.

In Table 1, Th is a threshold satisfying $\int \mathrm{MTF}(u,W_{20}=0,P)\mathrm{d}u \geqslant \mathrm{Th}$, where MTF denotes the modulation transfer function and P represents the mask parameters. The less sensitive the OTF is to defocus, the smaller will be the corresponding MTF. A very small MTF could cause difficulty in digital image restoration. Thus, Th is used to avoid this problem and ensure that the MTF will not be too small during the optimization. At the same time, Th is also a criterion based on which the performance of different phase masks can be assessed; having the same Th indicates that the MTF degradation is at the same level.

With the optimum mask parameters, the defocused 3D MTF can be computed, as shown in Fig. 1, where Th is set to 0.31 as an example. The MTF remains nearly unchanged when the defocus constant changes from 0 to 30. Figures 2 and 3 explain the importance of Eq. (8). In Figs. 2(a) and (b), Th is set to 0.21 and 0.25, and W_{20} is within the range of 0 to 30. The MTF curves are clearly quite stable no matter what the value of W_{20} is, proving that the system is defocus invariant. Figures 2(c) and (d) display the distribution of Eq. (8) corresponding to the

Table 1. Optimum Parameters of Sinusoidal Phase Mask

Th	α	ω	θ
0.21	395.76	1.37	0.0430
0.23	186.88	1.63	0.0798
0.25	239.91	1.44	0.0600
0.27	645.36	0.96	0.0499
0.29	186.89	1.41	3.0680
0.31	117.90	1.63	0.0779
0.33	67.890	1.84	3.0080
0.35	78.720	1.68	0.2230

optimum parameters, with the horizontal axis denoting the range of defocus and the vertical axis representing the range of normalized spatial frequency. Almost all the area has been covered as long as the mask is optimized and Eq. (8) is satisfied. Figure 3, in which θ is set to non-optimum values, is also provided for comparison. As Figs. 3(a) and (b) indicate, the defocused MTF are still stable with respect to the defocus aberration. However, the effective bandwidth of MTF decreases, corresponding to Figs. 3(c) and (d), where the effective area has been significantly reduced. The θ change for Th=0.21 is bigger than that for Th=0.25, thus the effective area for Th=0.21 becomes much smaller. A similar phenomenon will occur if we use non-optimum a/ω to plot Eq. (8), and thus the results are not given here. Equation (8) is therefore a necessary condition that should be satisfied for the sinusoidal phase mask to be capable of extending the DOF.

As the cubic type is the most popular phase mask, a performance comparison between the sinusoidal and cubic phase mask should be performed. The cubic phase mask is first optimized with the same optimization procedure as above. The comparison is then carried out with Th set at the same value. The Fisher information is also used to judge which type of phase mask is even less sensitive to defocus. Figure 4 shows the results.

Figure 4 shows that the Fisher information of the sinusoidal phase mask is not monotonic, with a seemingly global minimum around moderate defocus. The smaller the Fisher information is, the less sensitive will be the system to defocus. For smaller defocus values, the cubic phase mask is less sensitive to focus errors; meanwhile, for higher defocus values, the sinusoidal phase mask has a higher tolerance to misfocus. Because high defocus values can lead to the loss of high-frequency information, the standard sinusoidal phase mask performs slightly better than the cubic type, especially when the Th increases.

Numerical evaluations have proven that the standard sinusoidal phase mask can enlarge the DOF, but experimental results are more persuasive. First, a doublet with focal length of 50 mm and diameter of 30 mm is chosen as the primary imaging lens. In addition, Mintron CCD camera with 720 × 576 (pixels) resolution is used to record the images within the 380–780-nm spectral range. Second, the standard sinusoidal phase mask (15 × 15 × 3 (mm)) is fabricated using PMMA as the material and the mask parameters corresponding to those for use Th=0.25 (α = 239.91, ω = 1.44, and θ = 0.06). The real element and its 2D phase profiles are shown in Fig. 5. As a non-rotationally symmetric element, at least

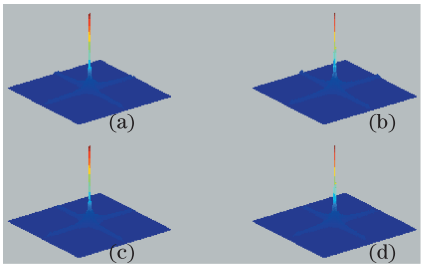

Fig. 1. Defocused MTF with Th set to 0.31 and defocus equaling (a) 0, (b) 10, (c) 20, and (d) 30.

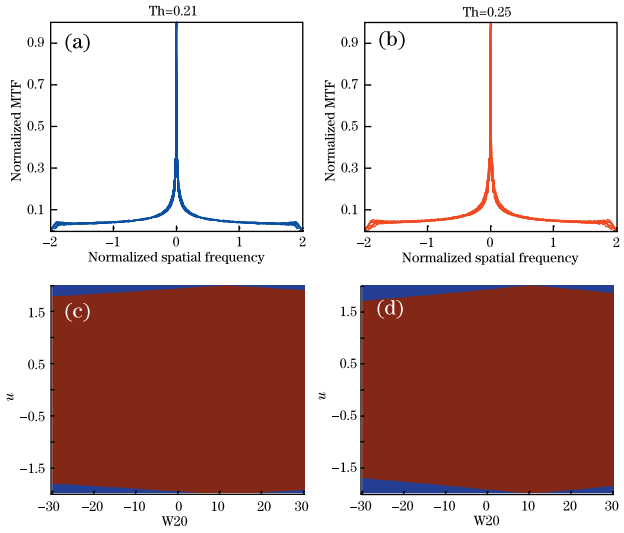

Fig. 2. Defocused MTF and visualization of Eq. (8) corresponding to the optimum parameters when Th is set to 0.21 and 0.25, respectively (the red area means that the condition of Eq. (8) is satisfied and the blue area indicates Eq. (8) is violated).

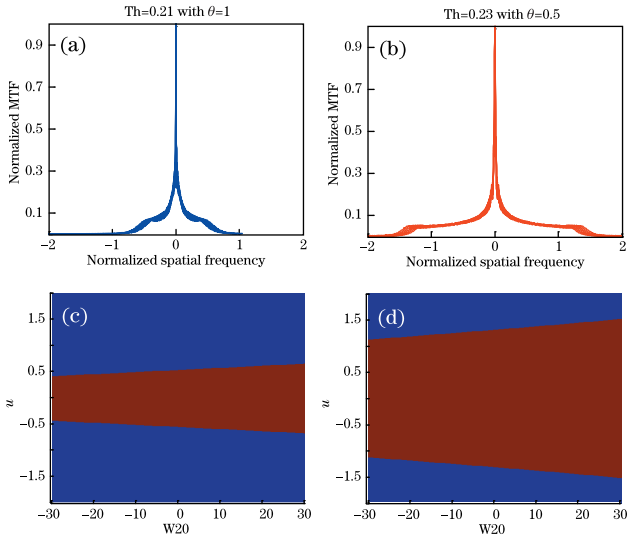

Fig. 3. Defocused MTF and visualization of Eq. (8) corresponding to the non-optimum parameters when Th is set to 0.21 and 0.25, respectively (the red area means that the condition Eq. (8) is satisfied and the blue area indicates Eq. (8) is violated).

0.1 μm of surface fabrication accuracy must be achieved to ensure the characteristics of the phase mask.

A lens tube is designed to fix the doublet and the phase mask, and the position of the focal plane cannot be changed. In this case, an ideal object plane is located about 330 mm away from the entrance pupil. Therefore, the effective F/# is approximately 3.3, and the original DOF is only about 1.5 cm. This small DOF makes it much easier to verify the DOF extension effect. Two groups of experiments are carried out and discussed.

First, a resolution chart is moved from –75 to 40 mm in a step of 10 mm, with the ideal object plane considered

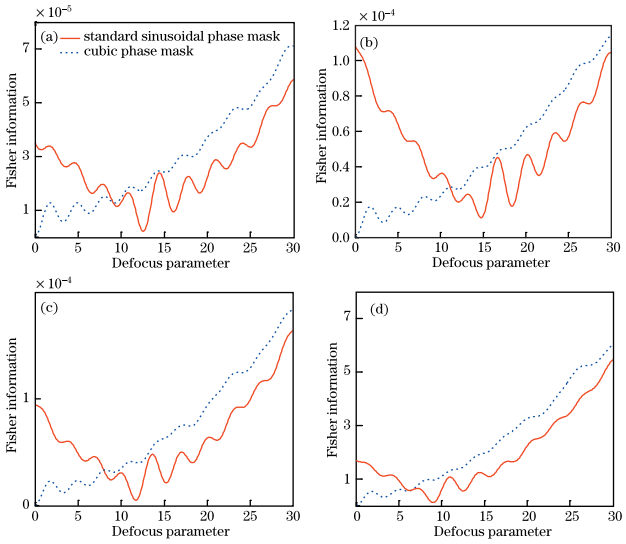

Fig. 4. Comparison of the defocus invariance between the cubic phase mask and the standard sinusoidal phase mask using Fisher information as a criterion with Th equaling (a) 0.21, (b) 0.23, (c) 0.25, and (d) 0.31, respectively.

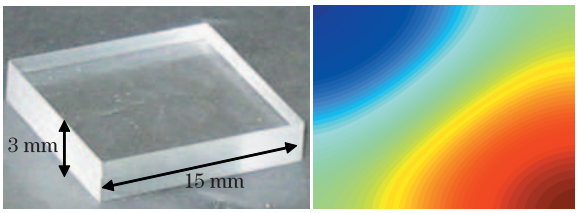

Fig. 5. Sinusoidal phase mask fabricated (left) and its 2D phase profiles (right).

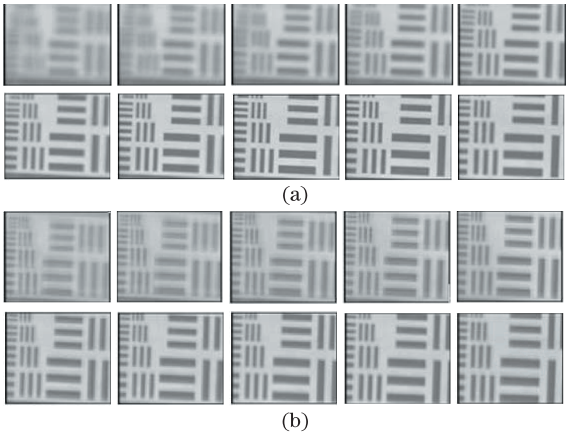

Fig. 6. Experimental results of the first group: (a) image series captured using only the doublet lens and (b) intermediate image captured with the sinusoidal phase mask added to the system aperture.

Fig. 7. Experimental results of the second group: (a) low DOF image; (b) intermediate image captured by the system with the sinusoidal phase mask added; and (c) restored large DOF image.

as the zero position. A series of images is captured to demonstrate the DOF extension effect, as shown in Fig. 6. The images in the left side of Fig. 6 correspond to the case in which no phase masks are used, while those in the right side are captured with the sinusoidal phase masks adopted. Only partial images captured around the ideal object plane are clear due to the small DOF. In addition, significant information loss can be seen at the extreme position. However, although the images demonstrate a uniform blur, which should be digitally eliminated, all the information can be resolved in the wavefront coding system. In addition, the ratio of DOF extension can be estimated at about 7.6.

Second, a textbook cover with the smallest spatial feature of 2 mm is titled to simulate one extended object. Moreover, the letter "B" is adjusted to be around the ideal object plane, as shown in Fig. 7, where the first row denotes the small DOF image and the second row is the image captured by the wavefront coding system. From the left-most part to the right-most part of the image, the variation of the defocus aberration constant is approximately $[-3.9\pi, 5.4\pi]$ with the ideal object plane as the zero reference position. Clearly, the parts that cannot be seen in the small DOF image reappears with the help of phase mask. This proves that the DOF is indeed extended. Although the information is preserved, the intermediate images are blurred, and digital restoration is necessary to obtain clear, large DOF images. The third row provides an example in which the popular Wiener filter is used to de-blur the images.

In conclusion, both the numerical analysis and experiments indicate that the standard sinusoidal phase mask is another alternative in extending the DOF.

This work was supported by the West Light Foundation of the Chinese Academy of Sciences under Grant No. J11-002.

References

1. E. R. Dowski, Jr. and W. T. Cathey, Appl. Opt. **34,** 1859 (1995).
2. Q. Yang, L. Liu, and J. Sun, Opt. Commun. **272,** 56 (2007).
3. S. S. Sherif, W. T. Cathey, and E. R. Dowski, Appl. Opt. **43,** 2709 (2004).
4. H. Zhao, Q. Li, and H. J. Feng, Opt. Lett. **33,** 1171 (2008).
5. W. Chi and N. George, Opt. Lett. **26,** 875 (2001).
6. M. Somayaji and M. P. Christensen, Appl. Opt. **46,** 216 (2007).
7. A. Sauceda and J. Ojeda-Castañeda, Opt. Lett. **29,** 560 (2004).
8. R. Barakat and A. Houston, Appl. Opt. **5,** 1850 (1966).
9. K. Kubala, E. Dowski, and W. Cathey, Opt. Express **11,** 2102 (2003).
10. W. T. Cathey and E. R. Dowski, Appl. Opt. **41,** 6080 (2002).
11. D. Robinson and D. G. Stork, in *Proceedings of Computational Optical Sensing and Imaging 2009* CThB3 (2009).
12. H. Zhao and Y. Li, Opt. Lett. **35,** 267 (2010).
13. Q. Liu, T. Zhao, Y. Chen, W. Zhang, and F. Yu, Chin. Opt. Lett. **8,** 159 (2010).
14. M. Born and E. Wolf, *Principle of Optics* (Pergamon Press, Oxford, 1985).